Journal of the American Heart Association

ORIGINAL RESEARCH

Loss of Type 2 Bone Morphogenetic Protein Receptor Activates NOD-Like Receptor Family Protein 3/Gasdermin E-Mediated Pyroptosis in Pulmonary Arterial Hypertension

Xiao-ting Tian, MS*; Zhou-yang-fan Peng, MS*; Yu-si Wu, PhD*; Yuan-yuan Cao, MS; Xue-chun Li, MD; Ying Li, MD, PhD; Si-Yuan Tang, MD, PhD; Alex F. Chen, MD, PhD; Xiao-hui Li, MD, PhD

BACKGROUND: Pulmonary arterial hypertension (PAH) is an incurable disease initiated by endothelial dysfunction, secondary to vascular inflammation and occlusive pulmonary arterial vascular remodeling, resulting in elevated pulmonary arterial pressure and right heart failure. Previous research has reported that dysfunction of type 2 bone morphogenetic protein receptor (BMPR2) signaling pathway in endothelium is inclined to prompt inflammation in PAH models, but the underlying mechanism of BMPR2 deficiency-mediated inflammation needs further investigation. This study was designed to investigate whether BMPR2 deficiency contributes to pulmonary arterial hypertension via the NLRP3 (NOD-like receptor family protein 3)/GSDME (gasdermin E)-mediated pyroptosis pathway.

METHODS AND RESULTS: NLRP3 knockout or short hairpin RNA interference of GSDME was performed in PAH animal models to investigate its effect on PAH progression. In addition, the effects of BMPR2 deficiency and restoration of BMPR2 by BMP9 (bone morphogenetic protein 9) or FK506 on pyroptosis were explored both in animal and cell models. Knockout of NLRP3 or short hairpin RNA interference of GSDME in animal models can alleviate the development of pyroptosis, accompanied with improved endothelial integrity, vascular remodeling, and right ventricular systolic pressure. Blocking BMPR2 is sufficient to induce NLRP3 upregulation and release of inflammatory factor IL-1β (interleukin-1β) in pulmonary arterial endothelial cells. Moreover, BMPR2 deficiency can induce GSDME-mediated pyroptosis through NLRP3 activation in 2 animal models, whereas activation of BMPR2 signaling by FK506 or BMP9 can reverse these phenotypes.

CONCLUSIONS: These findings provide evidence that loss of BMPR2 signaling promotes endothelial cell pyroptosis by enhancing NLRP3/GSDME signaling in PAH. Our findings may provide new insights to explore the inflammatory mechanism of PAH treatment.

Key Words: BMPR2 ■ GSDME ■ NLRP3 ■ pulmonary arterial hypertension ■ pyroptosis

Pulmonary arterial hypertension (PAH) is a rare disease characterized by endothelial cell (EC) dysfunction and excessive smooth muscle cell proliferation to induce occlusive vascular remodeling.[1,2] These pathological changes further trigger pulmonary flow resistance and progressive right heart failure.[3] Loss of type 2 bone morphogenetic protein receptor (BMPR2) is responsible for the

Correspondence to: Xiaohui Li, Department of Pharmacology, Xiangya School of Pharmaceutical Sciences, Central South University, 172 Tongzipo Road, Changsha, Hunan 410013, P. R. China. Email: xiaohuili@csu.edu.cn and Alex F. Chen, The Center for Vascular Disease and Translational Medicine, The Third Xiangya Hospital, Central South University, 138 Tongzipo Road, Changsha 410013, Hunan, China. Email: chenfengyuan@xinhuamed.com.cn

*X.-T. Tian, Z.-Y.-F. Peng and Y.-S. Wu contributed equally to this work.

This article was sent to Yen-Hung Lin, MD, PhD, Associate Editor, for review by expert referees, editorial decision, and final disposition.

For Sources of Funding and Disclosures, see page 15.

JAHA is available at: www.ahajournals.org/journal/jaha

RESEARCH PERSPECTIVE

What Is New?

- GSDME (gasdermin E) promotes the progression of pulmonary arterial hypertension (PAH) through pyroptosis, and GSDME knockdown can attenuate PAH.
- The NLRP3 (NOD-like receptor family protein 3) knockout alleviates endothelial dysfunction and PAH by suppressing GSDME-mediated pyroptosis pathway.
- NLRP3/GSDME can be regulated by type 2 bone morphogenetic protein receptor, and downregulation of type 2 bone morphogenetic protein receptor activates NLRP3/ GSDME-mediated endothelial pyroptosis, thereby contributing to the promotion of PAH.

What Question Should Be Addressed Next?

- The specific regulatory interactions between type 2 bone morphogenetic protein receptor and NLRP3/GSDME necessitate further investigation.
- Clinical translational value needs to be further confirmed, whether the expression of NLRP3 and GSDME are changed in patients with PAH, and whether NLRP3/GSDME can be targeted to intervene the progression of PAH.

Nonstandard Abbreviations and Acronyms

BMP	bone morphogenetic protein
BMPR2	type 2 bone morphogenetic protein receptor
GSDME	gasdermin E
HMGB1	high mobility group protein B1
MCTP	monocrotaline pyrrole
NLRP3	NOD-like receptor family protein 3
PAECs	pulmonary arterial endothelial cells
PAH	pulmonary arterial hypertension
SD	Sprague–Dawley
shRNA	short hairpin RNA

initiation and progression of hereditary PAH and a proportion of idiopathic PAH.[4] Previous studies have shown that conditional deletion of BMPR2 in the endothelium is sufficient to induce PAH[5] and restoration of endothelial BMPR2 expression reverses experimental pulmonary hypertension.[6,7] Additional studies have identified a role for endothelial BMPR2 loss in the exacerbation of vascular permeability and the altered translocation of leukocytes across the vascular wall.[8] Despite this evidence, the exact mechanism of endothelial BMPR2 signaling in the pathobiology of PAH remains uncertain.

PAH is strongly associated with inflammatory and immune components.[9] Pathological examination revealed that a large number of inflammatory cells infiltrated the pulmonary vascular occlusive area of patients with PAH.[10] Moreover, our and other previous studies have found that plasma levels of inflammatory factors such as HMGB1 (high mobility group protein B1), IL-1β (interleukin-1β) and TNF-α (tumor necrosis factor α) are significantly elevated, which is closely related to reduced survival rates.[9] Hence, anti-inflammatory treatment is considered to be one of the most promising approaches to treat PAH.[11,12] Recent studies have shown that loss of BMPR2 signaling induces an inflammatory response leading to the development of PAH.[13] BMPR2 gene mutations are associated with higher levels of IL-1β and HMGB1 in patients with PAH compared with patients who are nonmutated.[14] However, the specific mechanism by which the deficiency of BMPR2 signaling pathway inflames the inflammatory response remains unclear.

The NLRP3 (NOD-like receptor family protein 3) inflammasome plays an important role in the pathogenesis of several kinds of diseases by releasing a large number of inflammatory factors such as IL-18, IL-1β, and HMGB1.[15] HMGB1 and IL-1β are important inflammatory factors that play a role in the inflammatory response. Hence, we speculated that NLRP3 may be a key target of BMPR2 to participate in the development of PAH.

Activated NLRP3 induces the development of pyroptosis, which is a faster and more severe type of programmed cell death than apoptosis.[16] Pyroptosis has been defined as a gasdermin-dependent cell death; the most important pathological feature of pyroptosis is the destruction of cell structure and severe inflammatory response.[17] There are 2 main steps in the occurrence of pyroptosis. One is the formation of cell membrane pores, and another is the activation and release of inflammatory factors. The formation of cell membrane pores is mainly performed by active N-terminal fragment of GSDMD (gasdermin D) or GSDME (gasdermin E).[18] The study further found that activation of GSDME can rapidly transfer cells from apoptosis to pyroptosis and induce inflammation. When knocking down the GSDME expression, the cellular pyroptosis process was blocked.[19] Therefore, the expression level of GSDME is a hallmark of pyroptosis. Our previous study found that Caspase-4/11–mediated PAEC pyroptosis contributes to PAH.[20] However, whether blocking pyroptosis can reverse the development of PAH is still unknown.

Here, we speculate that knockout of NLRP3 or short hairpin RNA (shRNA) interference of GSDME can

attenuate the development of PAH in animal models. Downregulation of BMPR2 signaling activates PAEC pyroptosis via the NLRP3/GSDME pathway, thereby promoting endothelial injury and inflammatory response. Our study helps to elucidate the mechanism by which BMPR2 deficiency leads to PAH, which focuses on endothelial dysfunction and inflammatory response, providing a potential target for the exploration of anti-inflammatory treatments in PAH.

METHODS

The data supporting this study's findings are available from the corresponding author upon reasonable request.

Animal Experiments

Both male Sprague–Dawley (SD) rats (weighing 180–200 g, at age of 6–8 weeks) and C57BL/6 mice (weighing 20–22 g, at age of 8 weeks) were purchased from Hunan Jingdaslake Company and NLRP3$^{-/-}$ mice (weighing 22–25 g, at age of 8–12 weeks) were provided by Professor Lu Ben. These rats and mice were raised in the Department of Zoology of Hunan Normal University in accordance with the Institutional Animal Care and Use Committee. These animals were allowed free access to food and drinking water. All the animal experimental protocols were permitted by the Animal Ethics Committee of Hunan Normal University. All animals were grouped randomly, the sample size for animal experiments is based on our previous published articles,[14,20] animals that died during the PAH modeling were excluded, and a blind test was conducted in the animal experimental procedures.

Hypoxia-PAH Rat and Mice Model

SD rats were randomly placed in the normoxia (21% oxygen) or hypoxic (10% oxygen) chamber (Aipu Instrument Equipment Co., Ltd) for 21 days respectively. C57BL/6 mice and NLRP3$^{-/-}$ mice were randomly divided into 3 groups: wild type C57BL/6 mice in normoxia group (WT), WT C57BL/6 mice in hypoxia group (WT + hypoxia), and NLRP3$^{-/-}$ mice in hypoxia group (NLRP3$^{-/-}$ + hypoxia); mice were exposed to normoxia or hypoxia for 21 days. Normoxia rats and mice were kept in the same room adjacent to the hypoxic chamber.

Monocrotaline-PAH Rat Model

Pharmacological Activation of BMPR2

FK506 (tacrolimus) is used as a BMPR2 activator. The rats were randomly divided into 3 groups: control group, monocrotaline group (monocrotaline + vehicle), and monocrotaline with FK506 group (monocrotaline + FK506). Monocrotaline-treated rats were intraperitoneally injected with monocrotaline (60 mg/kg, Sigma-Aldrich, USA) once. After 3 weeks, rats in the monocrotaline + FK506 group were given 3 weeks of daily IP injections with 0.05 mg/kg/d FK506 (Sigma-Aldrich, USA). The control group was given intraperitoneal injections with solvent as vehicle control.

GSDME Lentivirus Gene Prevention

The method of lentivirus gene prevention in rat lung was performed as described before.[21–23] The SD rats (80–100 g) were randomly divided into 3 groups: control group, monocrotaline group (scramble shRNA+monocrotaline), monocrotaline with GSDME shRNA group (GSDME shRNA+monocrotaline), GSDME shRNA+monocrotaline group and scramble shRNA+monocrotaline group received lentivirus (2×10^7 Tu) containing GSDME shRNA (5′-GCTGGAGGAGACCTGATTTCA-3′) or scramble shRNA (5′-TTCTCCGAACGTGTCACGT-3′) (Genechem, China) in a single orotracheal dose. After 10 days, monocrotaline-treated rats were given intraperitoneal injections of MCT (60 mg/kg) to induce pulmonary hypertension. Control rats were given intraperitoneal injections with solvent as vehicle control. Animals were euthanized on day 21 after monocrotaline injections.

SU-5416-Hypoxia-PAH Rat Model

Pharmacological Activation of BMPR2

The SD rats were randomly divided into 3 groups: Control group, Sugen5416/hypoxia group (S/H + vehicle), and Sugen5416/hypoxia with FK506 group (S/H + FK506). Sugen5416/hypoxia treated rats were given a single subcutaneous dose of Sugen5416 (20 mg/kg, Selleck, USA) and then placed in hypoxic chamber (10% oxygen) for 3 weeks, followed by a period of 5 weeks normoxia. At the 8-week time point, the rats of S/H + FK506 group were given 3 weeks of daily intraperitoneal injections with 0.05mg/kg/d FK506. The control group was given intraperitoneal injections with solvent as vehicle control.

GSDME Lentivirus Gene Prevention

The SD rats (80–100 g) were randomly divided into 3 groups: Control group, Sugen5416/hypoxia group (scramble shRNA+S/H), and Sugen5416/hypoxia with GSDME shRNA group (GSDME shRNA+S/H). The GSDME shRNA+S/H group and scramble shRNA+S/H group received lentivirus (2×10^7 Tu) containing GSDME shRNA or scramble shRNA in a single orotracheal dose. After 10 days, Sugen5416/hypoxia treated rats were given a single subcutaneous dose of Sugen5416 (20 mg/kg, Selleck, USA) and then placed in hypoxic chamber (10% oxygen) for 3 weeks,

followed by a period of 5 weeks normoxia. Control rats were given intraperitoneal injections with solvent as vehicle control. Animals were euthanized on day 56 after Sugen5416 injection.

Hemodynamic Evaluation

At the end of the experiment, hemodynamic parameters were evaluated. Briefly, animals were anesthetized with pentobarbital sodium (65 mg/kg BW i.p.). The right ventricular (RV) systolic pressure was detected by right heart catheter (Smiths Medical, UK) and recorded by TM-WAVE. The heart was isolated, and the RV hypertrophy was assessed by calculating RV weight versus left ventricular plus septum weight.

Immunofluorescence

The tissue sections were placed in a box containing EDTA antigen retrieval buffer (pH 8.0) and placed in a microwave oven for antigen retrieval. After cooling, they were washed with PBS and incubated with an autofluorescence quencher for 5 minutes, and then washed with water for 10 minutes. After BSA was added dropwise for 30 minutes, the primary antibody anti-NLRP3 (GB114320, 1:200; Servicebio, China), anti-CD31 (GB11063-2, 1:200; Servicebio, China) was dropped and the overnight incubation was carried out at 4 °C in a refrigerator. On the second day, the slides of the primary antibody were washed with PBS, and the sections were immersed and dried, then the secondary antibody (GB21303, 1:300; GB22303,1:400; Servicebio, China) was added, and the slides were incubated for 50 minutes at room temperature in the dark. After washing with PBS, the slides were counterstained with DAPI (G1012-100ML; Servicebio, China) for 10 minutes. Finally, the antifluorescence quenching capsule was used for sealing. Images were acquired with a digital slice scanner (Panoramic MIDI, Panoramic 250FLASH, Panoramic DESK; 3DHISTECH, Hungary).

Hematoxylin and Eosin Staining

The lung tissue was immersed in 4% paraformaldehyde for fixation, and a paraffin section having a thickness of about 5 μm was prepared. The sections were placed on a glass slide and washed 3 times with PBS for 3 minutes each time. The sections were then placed in xylene for dewaxing and then immersed in anhydrous ethanol, 90% ethanol, 80% ethanol, and 70% ethanol at a high to low concentration for 5 minutes, then washed 3 times with distilled water. Finally, they were stained with hematoxylin for 5 minutes, washed with distilled water and 1% hydrochloric acid for 3 seconds, washed with distilled water for 15 seconds, and then washed with 80% ethanol, 90% ethanol, and absolute ethanol for 3 seconds from low to high concentration. Then, using xylene carbonate and xylene for 5 minutes and 2 minutes, the tablets were sealed with neutral gum.

Enzyme-Linked Immunosorbent Assay

The measurement of plasma concentration of inflammatory factor IL-1β was measured by ELISA kits (Proteintech, USA).

Cell Culture

The cells used in the experiment are human pulmonary arterial ECs (PAECs) purchased from American Type Culture Collection. The cells were cultured at 37 °C under 5% CO_2 in DMEM F12 containing 10% fetal bovine serum (Hyclone, USA).

Small Interfering RNA Transfection

Cells were transiently/stably transfected with BMPR2 small interfering RNA (siRNA) (Ribobio, China). The siRNA lyophilized powder was dissolved in RNase-free water to prepare a 5 nmol stock solution. The final transfection concentration was 50 nM. The method was as follows: dilute 5 μL of siRNA stock solution (20 μM) with Opti-MEM medium 120 μL for transfection, add 12 μL of HiPerFect Transfection Reagent, 2 mL medium, mix them gently. Incubate at room temperature for 15 minutes, then discard the prepared culture medium of the 6-well plate, wash it 3 times with PBS, then add the prepared siRNA mixture, and put it into the incubator for 72 hours.

Lactate Dehydrogenase Release Assay

According to the description: 20 μL of the lactic acid solution, 20 μL of INT solution (1×) and 20 μL of enzyme solution were mixed in the dark. The supernatant of the 6-well plate was separately aspirated, and after centrifugation, 120 μL of the supernatant was taken in a 96-well plate for each sample, and then 60 μL of the prepared LDH (lactate dehydrogenase) test solution

Figure 1. Pro-PAH factors hypoxia, MCTP, and TNF-α induce pyroptosis in PAECs.
A, Morphological changes of cells after the intervention of PAECs by hypoxia, MCTP, and TNF-α. Scale bar: 100 μm. **B**, TUNEL staining for apoptosis of cells after hypoxia, MCTP, and TNF-α intervention in human pulmonary arterial endothelial cells. **C–E**, Detection of LDH release after hypoxia (n=5), MCTP (n=5), and TNF-α (n=6) intervention in PAECs. **F–N**, Representative immunoblots of GSDME-N and Clev-IL-1β after treatment of PAECs with hypoxia (1% O_2), MCTP (31 μM), and TNF-α (40 ng/mL), n=4. Mann–Whitney test was used. Clev-IL-1β indicates Cleaved-interleukin-1β; GSDME, gasdermin E; LDH, lactate dehydrogenase; MCTP, monocrotaline pyrrole; PAEC, pulmonary arterial endothelial cell; PAH, pulmonary arterial hypertension; and TNF-α, tumor necrosis factor alpha.

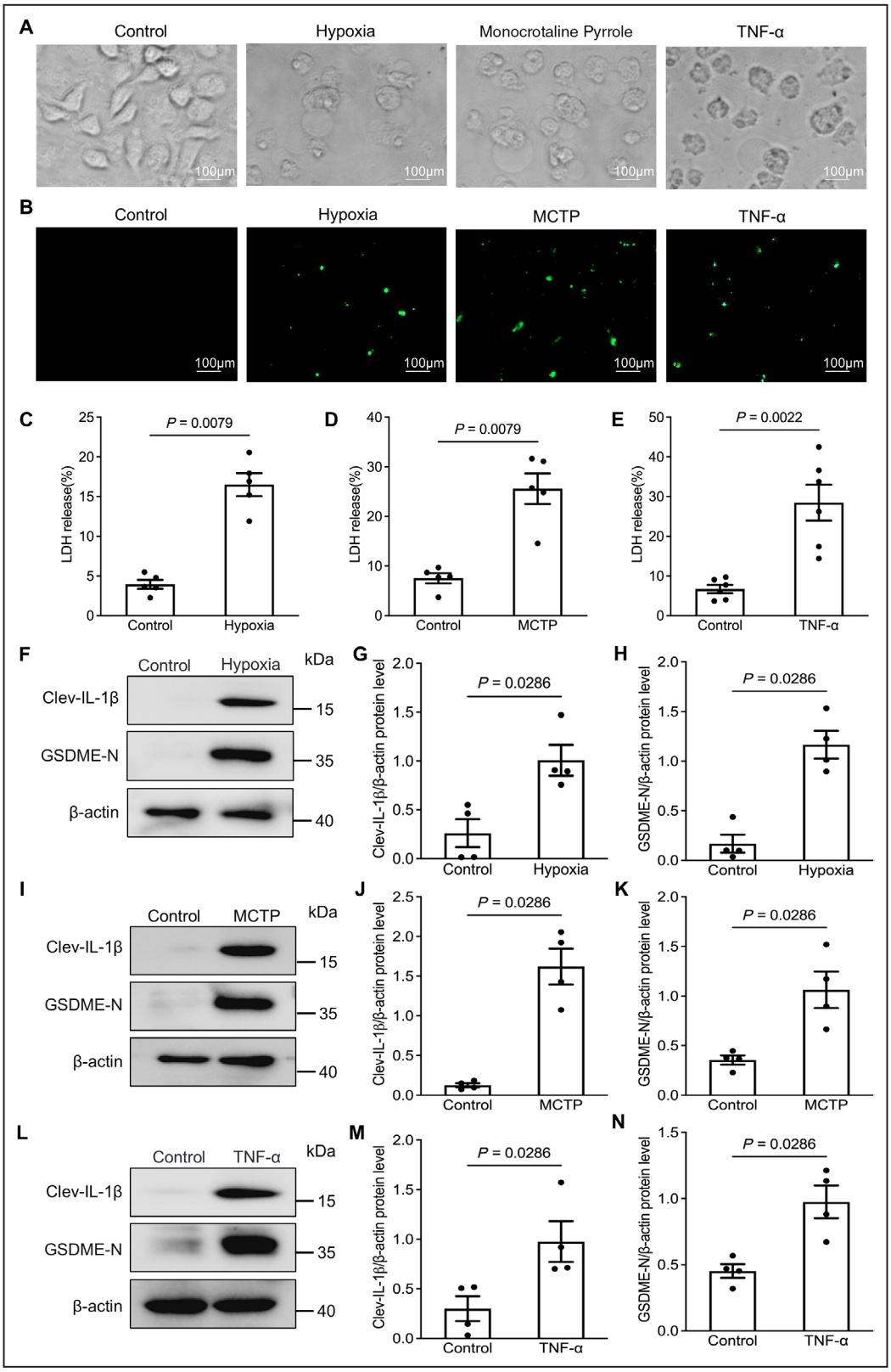

(Beyotime, China) was added to each well. The light was placed on a shaker for 30 minutes and then its absorbance was measured at a wavelength of 490 nm.

Tunel Assay

Tunel staining was accomplished using a TUNEL kit (Beyotime, China). The cell supernatant was discarded

and washed once with PBS. The cells were fixed with 4% paraformaldehyde for 30 minutes, washed with PBS, incubated with 0.3% Triton X-100 for 5 minutes at room temperature, washed twice with PBS, and then added to each well in a 6-well plate. A 100 μL Tunel test solution was incubated at 37 °C for 60 minutes in the dark. The PBS was washed 3 times and observed under a fluorescence microscope.

Western Blotting

Protein extraction was used by PMSF lysate (RIPA:PMSF: protease inhibitor cocktail = 100:1:1),

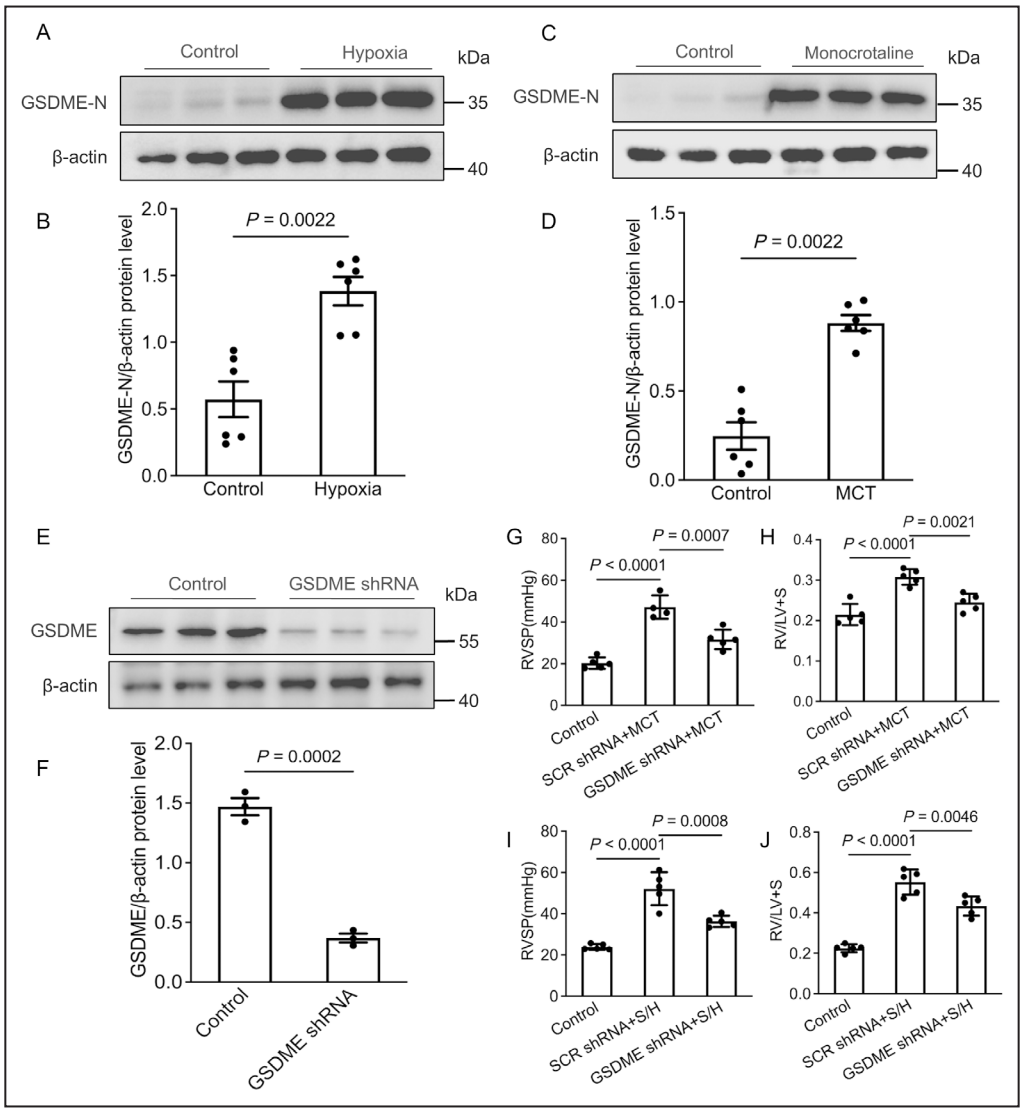

Figure 2. Inhibition of GSDME attenuates the development of experimental PAH in rats.
A, B, Representative immunoblots of GSDME-N in lung lysate of hypoxia-induced PAH rats, n=6. **C, D**, Representative immunoblots of GSDME-N in lung lysate of monocrotaline-induced PAH rats. **E–F**, Western blot result of GSDME after knockdown by lentivirus, n=3. **G, H**, RVSPmeasurements (**G**) and indices of RV/(LV + S) in Control, SCR shRNA+MCT, and GSDME shRNA+MCT rats (**H**). n=5. **I, J**, Bar charts showing the result of RVSP (**I**) and indices of RV/(LV + S) in Control, SCR shRNA+S/H, and GSDME shRNA+S/H groups (**J**). n=5. Mann–Whitney test was used for(**A–D**). Normal distribution was confirmed by the Shapiro–Wilk test, statistical analysis was performed using 1-way ANOVA followed by Tukey's test for (**E–J**). GSDME indicates gasdermin E; GSDME shRNA+MCT, gasdermin E short hairpin RNA+monocrotaline; LDH, lactate dehydrogenase; MCTP, monocrotaline pyrrole; PAEC, pulmonary arterial endothelial cell; PAH, pulmonary arterial hypertension; RV/(LV + S), right ventricle weight/left ventricle weight + ventricular septum; RVSP, right ventricle systolic pressure; SCR shRNA+MCT, scramble short hairpin RNA+monocrotaline; SCR shRNA+S/H, scramble short hairpin RNA+Sugen5416/hypoxia; and TNF-α, tumor necrosis factor alpha.

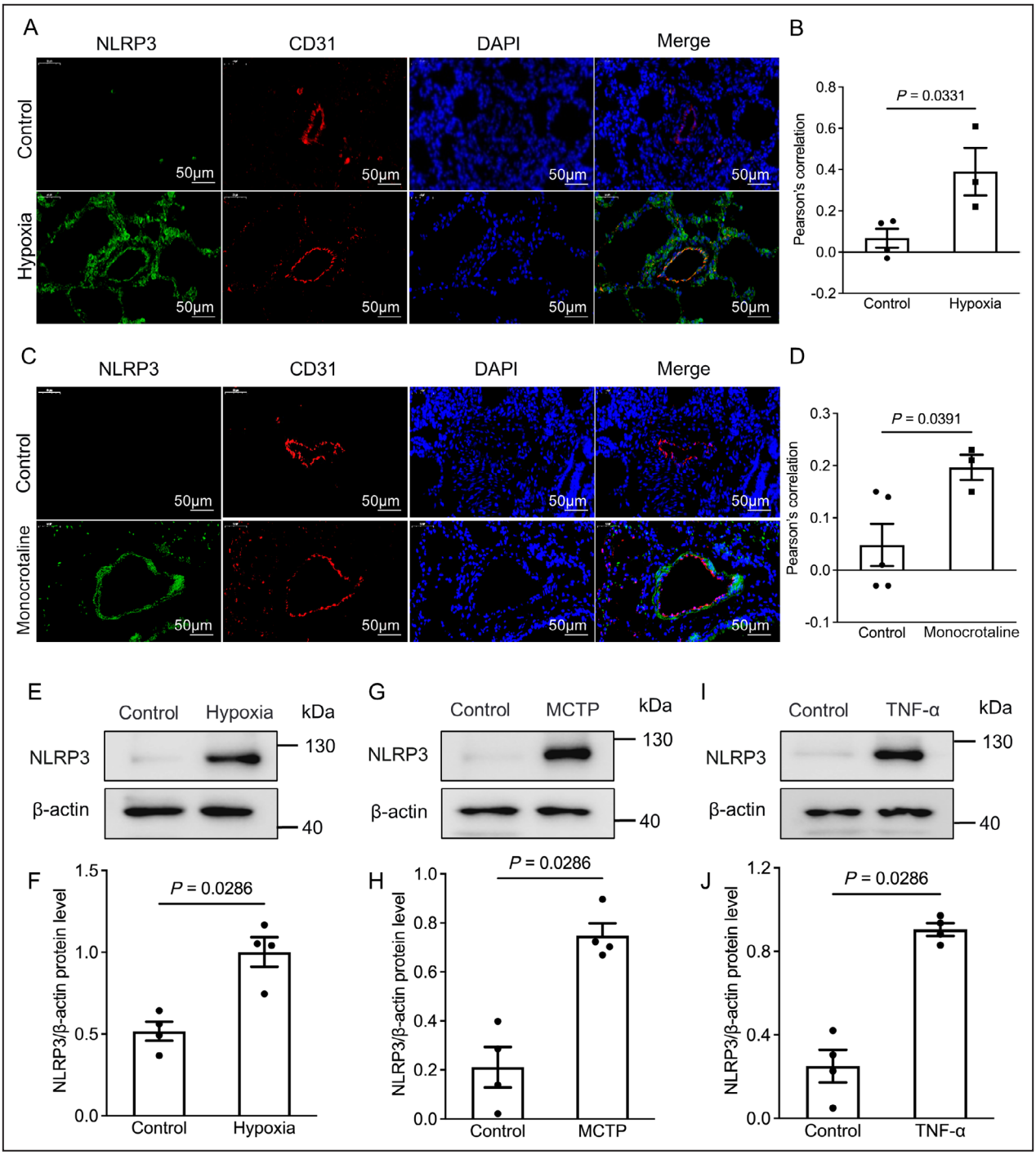

Figure 3. Upregulation of NLRP3 expression in PAH rat model and pro-PAH factors induced PAECs.
A, C, Expression position of NLRP3 in lung tissue sections of monocrotaline- and hypoxia-induced PAH rat models. **B, D**, Pearson's correlation between CD31 and NLRP3. **B**, Control group: n=4, Hypoxia group: n=3. **D**, Control group: n=5, monocrotaline group: n=3. CD31: endothelial marker; DAPI: nuclear marker. Normal distribution was confirmed by the Shapiro–Wilk test. Statistical analysis was performed using Student *t* test. **E–J**, Representative immunoblots of NLRP3 after incubation with hypoxia (1% O_2), MCTP (31 μM) and TNF-α (40 ng/mL) in PAECs; n=4. Statistical analysis was performed using Mann–Whitney test. MCTP indicates monocrotaline pyrrole; NLRP3, NOD-like receptor family protein 3; PAEC, pulmonary arterial endothelial cell; PAH, pulmonary arterial hypertension; and TNF-α, tumor necrosis factor alpha.

protein concentrations were measured by BCA Protein Assay Kit (Thermo Scientific, Rockford, IL). Equal amounts of protein from each sample (50 μg) were separated by 8% sodium dodecyl sulfate-polyacrylamide gel electrophoresis (SDS-PAGE) and 12% SDS-PAGE transferred to polyvinylidene fluoride membranes. After incubated with 5% milk for 1 hour at room temperature, the membranes were incubated with primary antibodies against NLRP3 (1:1000, Abcam, UK), GSDME (1:1000, Abcam, UK), BMPR2 (1:1000, Proteintech, USA), IL-1β (1:1000, Abcam, USA), and β-actin (1:5000, Proteintech, USA) overnight at 4 °C, followed by horseradish peroxidase-conjugated secondary antibodies (1:5000, Jackson Immunoresearch, USA) incubation. Then the PVDF membrane was soaked in the illuminating liquid and then exposed to the imager (BioRad, USA). After image scanning and processing using Image Lab software, the relative quantification of the target protein was performed by Image J software.

Statistical Analysis

Data in our study are presented as mean ± SEM. GraphPad prism (version 9.5.1) was used for the statistical analysis. The normality of the data distribution was assessed using the Shapiro–Wilk test. If the data conformed to a normal distribution, the comparisons between-group differences were calculated with Student's *t* test (2 groups), 1-way ANOVA followed by Turkey's or Newman Keuls multiple comparisons test (multiple groups). Kruskal–Wallis with Dunn's multiple comparison tests were used for nonnormally distributed variables. The detailed statistical analysis for each experiment is described in the respective figure legends. Statistical significance was reported at $P<0.05$.

RESULTS

Pro-PAH Factors Hypoxia, Monocrotaline Pyrrole, and TNF-α Induce Pyroptosis in PAECs

To explore whether pyroptosis occurred in PAH, PAECs were incubated with hypoxia, monocrotaline pyrrole (MCTP), and TNF-α to establish a model of pulmonary artery endothelial injury. Microscopic photographs showed obvious cell morphogenesis, cell punching, swelling, blistering, and rupture (Figure 1A). TUNEL staining showed that a large number of deaths occurred in hypoxia, MCTP, and TNF-α treated PAECs (Figure 1B). The release of LDH was detected by the LDH kit, and it was found that the release of LDH in the intervention group was significantly higher than that in the control group (Figure 1C–1E), suggesting massive cell death. Western blot showed that the protein expression of GSDME-N and inflammatory factor IL-1β were significantly upregulated (Figure 1F–1N), providing further confirmation of the occurrence of pyroptosis in PAECs.

Inhibition of GSDME Attenuates the Development of Experimental PAH in Rats

To detect the occurrence of pyroptosis in pulmonary hypertension rats, Western blot was used to detect the expression of GSDME-N in the lung tissue of rats with pulmonary hypertension induced by hypoxia and monocrotaline. It was found that the expression of GSDME-N was significantly increased compared with the control group (Figure 2A–2D), indicating that pyroptosis exists in hypoxic and monocrotaline induced pulmonary hypertension. Administration of rats with GSDME shRNA to clarify the role of GSDME-mediated pyroptosis in PAH (Figure 2E–2F). The results indicating that silencing GSDME is a sufficient way to block the development of pyroptosis. We created 2 experimental PAH models in rats after using shRNA and found that the GSDME shRNA group showed a significant reduction in RV systolic pressure and RV hypertrophy (Figure 2G–2J). These results support our hypothesis that inhibition of GSDME-mediated pyroptosis is sufficient to repress PAH.

Upregulation of NLRP3 Expression in PAH Rat Model and Pro-PAH Factors Induced PAECs

We constructed 2 rat models of pulmonary hypertension using hypoxia (10% O_2) and monocrotaline (60 mg/kg) separately. Immunofluorescence was used to detect the expression of NLRP3 on lung tissue sections. The results showed that the expression of NLRP3 on lung endothelial cells of rats with monocrotaline and hypoxic pulmonary hypertension was significantly

Figure 4. Knockout of the NLRP3 alleviates the progression of PAH and inhibits GSDME-mediated pyroptosis.
A, RVSP (n=5). **B**, RV/(LV + S) (n=6). **C**, ELISA result of IL-1β release in serum (WT group, n=6; WT + Hypoxia group, n=7; NLRP3−/− + Hypoxia group, n=5). **D, E**, Hematoxylin–eosin staining and the thickness of vascular wall. Arrows pointing to small and medium arteries. Scale bar:100 μm. **F–J**, Representative immunoblots of GSDME, GSDME-N, Pro-IL-1β, Clev-IL-1β, and NLRP3 in the WT group, WT + Hypoxia group, and $NLRP3^{-/-}$ + Hypoxia group. n=3. Normal distribution was confirmed by the Shapiro–Wilk test, statistical analysis was performed using 1-way ANOVA followed by Tukey's or Newman test. For (**J**), Kruskal–Wallis with Dunn's multiple comparison tests was used. Clev-IL-1β indicates cleaved interleukin-1β; GSDME, gasdermin E; NLRP3, NOD-like receptor family protein 3; PAH, pulmonary arterial hypertension; RV/(LV + S), right ventricle weight/left ventricle weight + ventricular septum; RVSP, right ventricle systolic pressure; and WT, wild type.

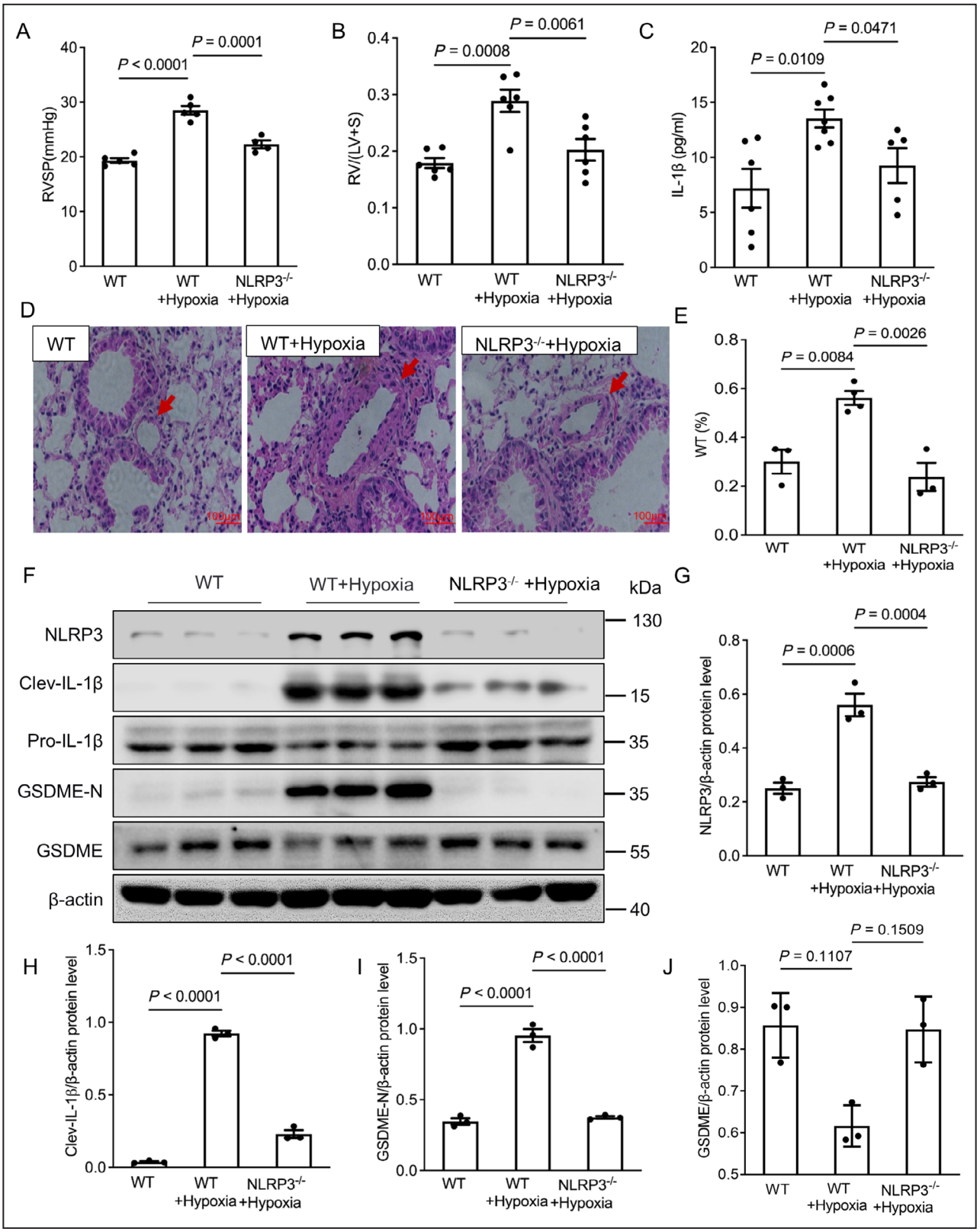

upregulated (Figure 3A–3D). This result provides evidence for our subsequent use of PAECs. Then PAECs were cultured with pro-PH factors hypoxia, MCTP, and TNF-α. After 24 hours, the protein was collected and detected by Western blot. The expression of NLRP3 was increased in PAECs treated with hypoxia,

MCTP, and TNF-α compared with the control group (Figure 3E–3J).

Knockout of the NLRP3 Alleviates the Progression of PAH and Inhibits GSDME-Mediated Pyroptosis

To further determine the relationship between NLRP3 and GSDME in pulmonary hypertension. We performed hypoxic-induced pulmonary hypertension in WT and NLRP3$^{-/-}$ mice and found pulmonary artery pressure was reduced in NLRP3$^{-/-}$ mice (Figure 4A), and RV hypertrophy and pulmonary artery remodeling were significantly alleviated in NLRP3$^{-/-}$ mice under hypoxic conditions (Figure 4B, 4D, 4E). ELISA results showed that the plasma level of IL-1β was significantly upregulated in hypoxic WT mice, whereas in the group of NLRP3$^{-/-}$ mice decreased (Figure 4C). Western blot was used to detect the expression of NLRP3, Clev-IL-1β (Cleaved-IL-1β), and GSDME-N in lung tissue of NLRP3$^{-/-}$ mice. It showed that the expression of NLRP3, Clev-IL-1β, and GSDME-N were significantly upregulated in hypoxic WT mice, and knockout of the NLRP3 gene reduced the expression of those pyroptosis-related proteins (Figure 4F–4J).

Activated BMPR2 Signaling Inhibits Pyroptosis in Experimental PAH Animal Models

BMPR2 plays an important role in pulmonary hypertension, which can induce the release of inflammatory factors. However, whether BMPR2 affects the expression of NLRP3 is unknown. FK506 (tacrolimus), a BMPR2 signaling agonist, can bind with a BMP (bone morphogenetic protein) signaling repressor, FKBP12 (FK-binding protein-12). FK506 treatment alleviates PAH in patients and experimental models by blocking the combination of FKBP12 and type I receptors activin receptor-like kinase to activate the downstream of BMPR2 signaling. We used monocrotaline or VEGF (vascular endothelial growth factor) receptor blocker Sugen5416 plus chronic hypoxia to establish experimental models and FK506 was administered at the indicated time point. The vehicle group showed severe PAH at the end of the experiment, whereas FK506 treatment significantly reduced PAH, as shown by the decreased RV systolic pressure (Figure 5A, 5C) and RV hypertrophy (Figure 5B, 5D). In PAH animals treated with FK506, the reversal of PAH progression was associated with a reduction of the pathological increases of N-GSDME (Figure 5E–5J). Immunofluorescence was used to detect the expression of NLRP3 in lung tissue. The results showed that the expression of NLRP3 on the pulmonary endothelial cells of rats with monocrotaline and hypoxic pulmonary hypertension was significantly upregulated. However, all these effects were reversed by the BMPR2 agonist FK506 (Figure 5K–5L). Thus, we suspect that BMPR2 affects the activation of NLRP3 and GSDME.

Restoring the BMPR2 Signaling Downregulate the NLRP3/GSDME Pathway in PAECs

Next, we used hypoxia, MCTP, and TNF-α to stimulate PAECs to reduce the expression of BMPR2 and restore the expression of BMP signaling pathway by using BMP9. The results implied that BMP9 could restore the increase of NLRP3, Clev-IL-1β, and GSDME-N due to the decreased expression of BMPR2 in PAECs (Figure 6A–6O).

BMP9 Reverses BMPR2 Signaling to Inhibit NLRP3 and GSDME in PAECs

To further determine the relationship between BMPR2 and NLRP3 signaling pathways in pulmonary hypertension. We silenced the BMPR2 protein in PAECs with siRNA and restored the expression of BMP signaling pathway using BMP9. Silencing was successfully compared with the negative control group, and NLRP3 was activated after BMPR2 silencing (Figure 7A–7C). Meanwhile, the expression of the pyroptosis-related protein was also detected, and it was found that GSDME was cleaved and GSDME-N was significantly increased (Figure 7D–7F) whereas BMP9 can inhibit its upregulation.

DISCUSSION

Our study provides the first evidence that loss of BMPR2 induces endothelial cell pyroptosis through

Figure 5. Activated BMPR2 signaling inhibits pyroptosis in experimental PAH animal models.
A, C, RVSP. **B, D**, RV/(LV+S). **A**, Control group, n=7; S/H+Vehicle group, n=6; S/H+FK506 group, n=7, **B**, n=6, **C**, Control group, n=6; monocrotaline+Vehicle group, n=6; monocrotaline+FK506 group, n=7, **D**, Control group, n=7; monocrotaline+Vehicle group, n=6; monocrotaline T+FK506 group, n=7. **E, G, H**, Representative immunoblots of BMPR2, GSDME-N expression in lungs lysate isolated from Control, Su5416+hypoxia, and Hypoxia/Su5416+FK506 groups, n=3. **F, I, J**, Representative immunoblots of BMPR2, GSDME-N expression in lungs isolated from Control, monocrotaline, and monocrotaline+FK506 groups, n=3. **K, L**, Expression position of NLRP3 in lung tissue sections. CD31: endothelial marker; DAPI: nuclear marker. Normal distribution was confirmed by the Shapiro–Wilk test, statistical analysis was performed using 1-way ANOVA followed by Tukey's or Newman test. BMPR2 indicates type 2 bone morphogenetic protein receptor; GSDME, gasdermin E; NLRP3, NOD-like receptor family protein 3; PAH, pulmonary arterial hypertension; RV/(LV+S), right ventricle weight/left ventricle weight+ventricular septum; and RVSP, right ventricle systolic pressure.

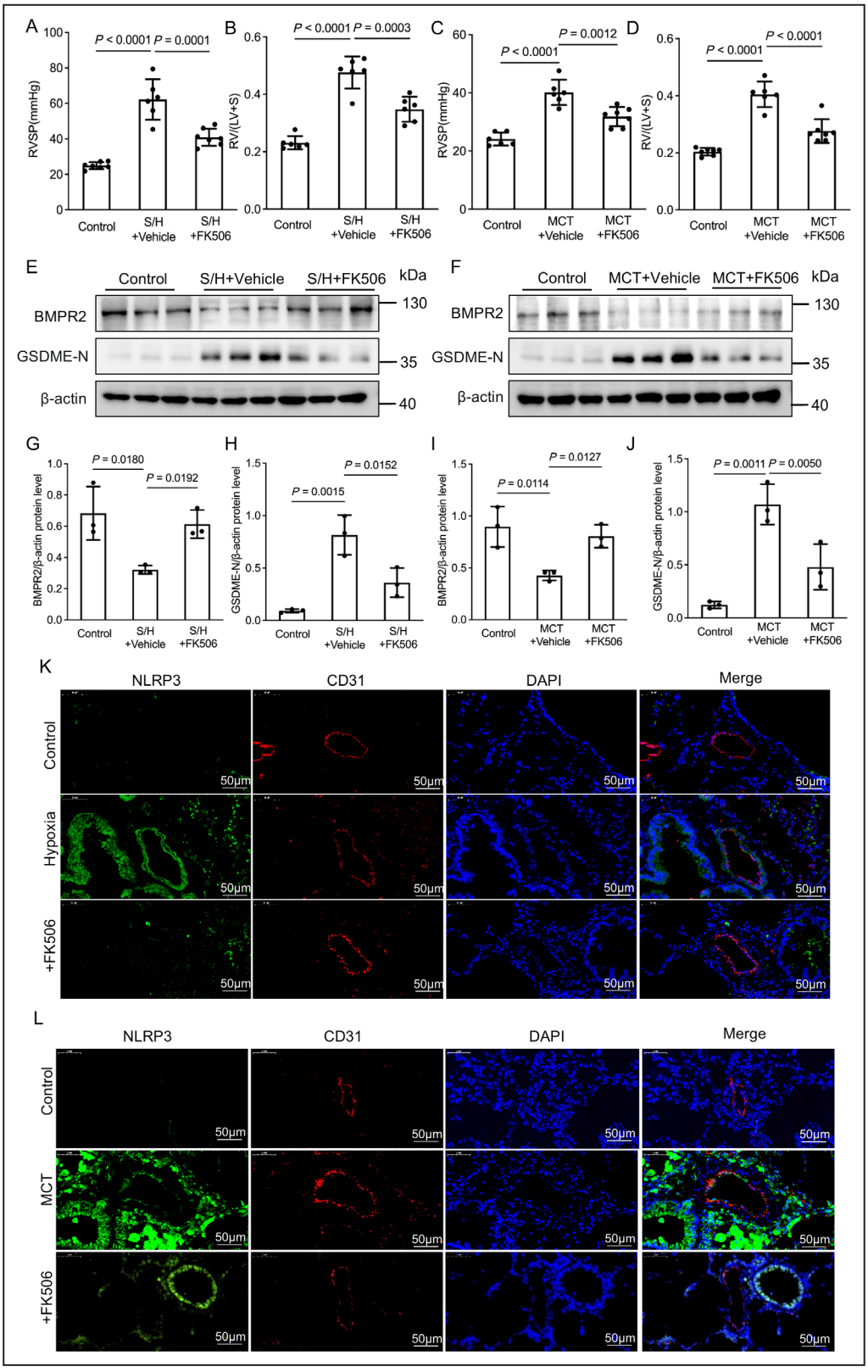

the NLRP3/GSDME pathway in PAH models. These findings are supported by solid results: (1) pyroptosis occurs in experimental PAH models, and knockdown of the pyroptosis executor GSDME can inhibit the development of PAH; (2) genetic ablation of NLRP3 inhibited the development of PAH via repressing GSDME-mediated pyroptosis; and (3) using BMPR2 activator FK506 or BMP9 can effectively repress

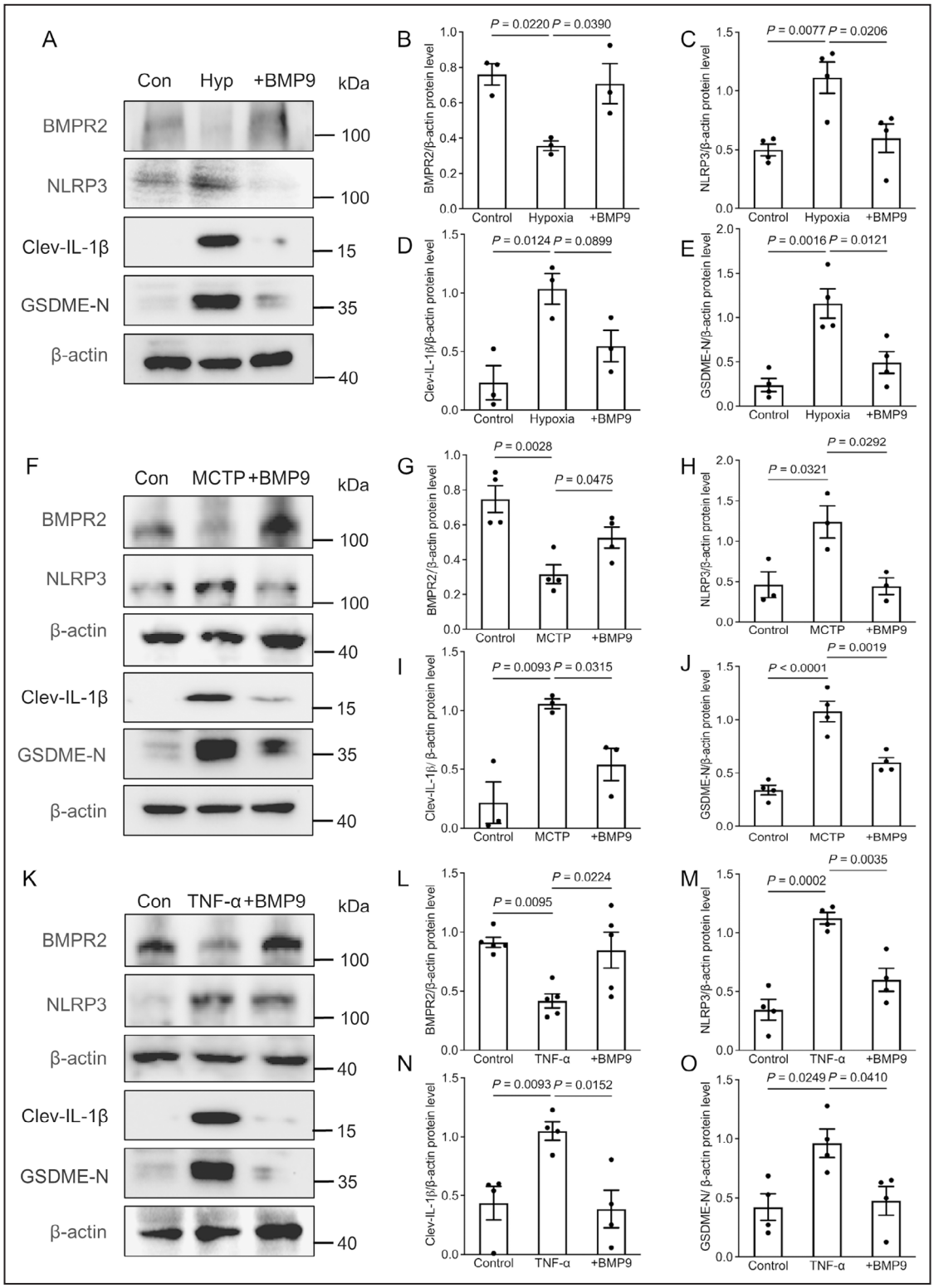

Figure 6. Restoring the BMPR2 signaling downregulates the NLRP3/GSDME pathway in PAECs.
PAECs were incubated with hypoxia, MCTP, and TNF-α with or without BMP9. **A, F, K**, Representative immunoblots of BMPR2, NLRP3, GSDME-N, and Clev-IL-1β expression. **B-E, G–J, L–O**, Quantitative analysis results of (**A, F, K**). **B, D, H, I**, n=3; **C, E, G, J, N, O**, n=4; **L, M**, n=5. Normal distribution was confirmed by the Shapiro–Wilk test, statistical analysis was performed using 1-way ANOVA followed by Tukey's or Newman test. BMPR2 indicates type 2 bone morphogenetic protein receptor; BMP9, bone morphogenetic protein 9; Clev-IL-1β, cleaved interleukin-1β; GSDME, gasdermin E; MCTP, MCTP, monocrotaline pyrrole; NLRP3, NOD-like receptor family protein 3; PAEC, pulmonary arterial endothelial cell; and TNF-α, tumor necrosis factor alpha.

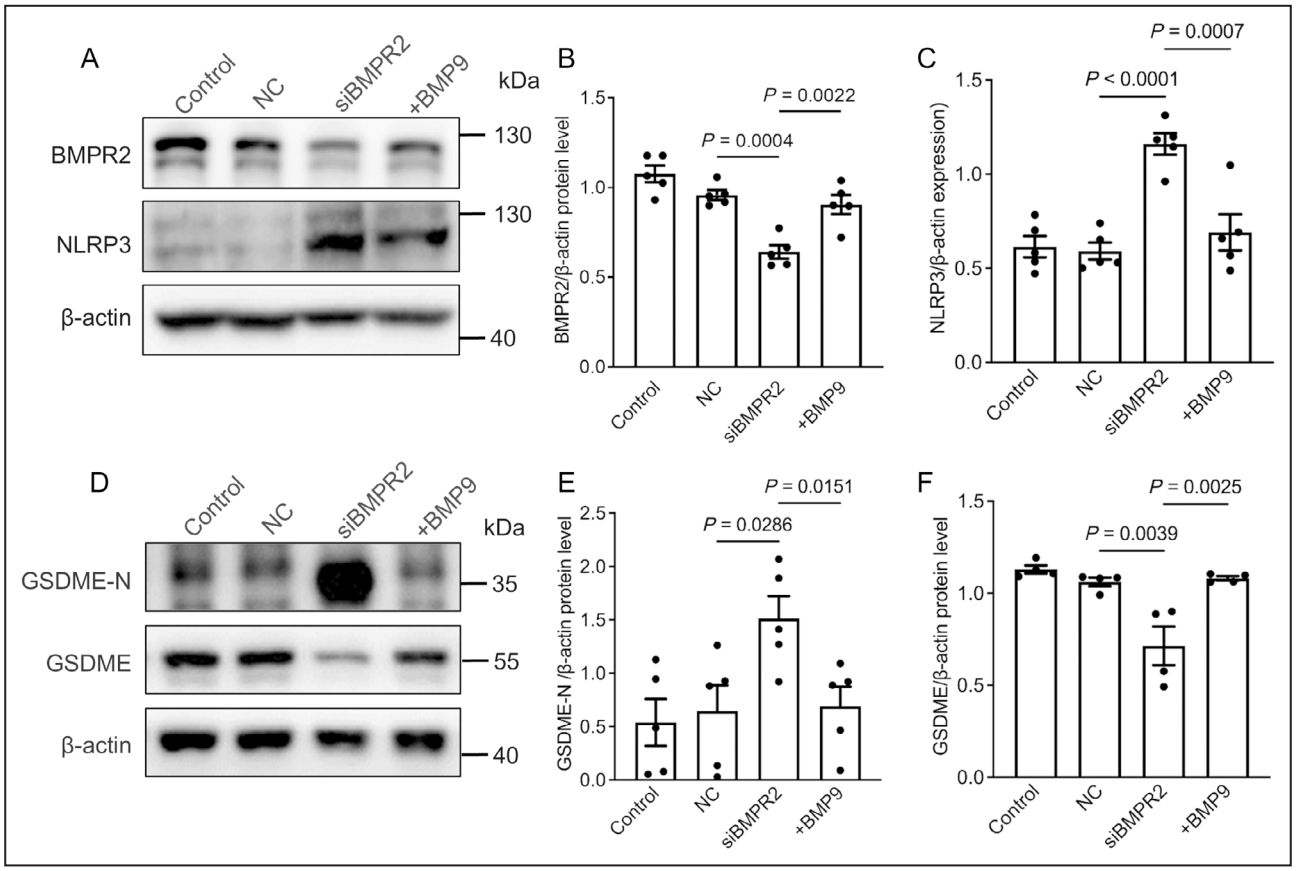

Figure 7. BMP9 reverses BMPR2 signaling to inhibit NLRP3 and GSDME in PAECs.
PAECs were treated with siBMPR2 and siBMPR2+BMP9. **A, D**, Representative immunoblots of BMPR2, NLRP3, GSDME and GSDME-N expression. **B, C, E, F**, Quantitative analysis results of (**A** and **D**). **B, C, E**, n=5; **F**, n=4. Normal distribution was confirmed by the Shapiro–Wilk test, statistical analysis was performed using 1-way ANOVA followed by Tukey's test. BMPR2 indicates type 2 bone morphogenetic protein receptor; BMP9, bone morphogenetic protein 9; GSDME, gasdermin E; NC, negative control; NLRP3, NOD-like receptor family protein 3; and PAEC, pulmonary arterial endothelial cell.

NLRP3 and GSDME activation to block the development of experimental PAH.

The NLRP3 inflammasome is an important mediator to release many inflammatory factors such as IL-18, IL-1β, and HMGB1, which have been proved to participate in several kinds of infectious diseases.[24–26] IL-1β and IL-18 are involved in the development of chronic obstructive pulmonary disease,[27] and these patients have increased levels of caspase-1 in the lung tissue,[10] indicating a role for the inflammasomes in the pathogenesis of obstructive pulmonary disease.[9] In our study, we found that knockout of NLRP3 can inhibit the progression of PAH and reduce the release of IL-1β, which is mediated by GSDME-mediated pyroptosis pathway, suggesting that knockout of NLRP3 can inhibit the inflammatory response via GSDME-mediated pyroptosis in PAH.

Pyroptosis is a newly identified type of programmed cell death that is mediated by gasdermin family members, such as GSDMD[28] or GSDME.[29] With the definition of pyroptosis being a gasdermin-driven cell death, the activation of pyroptosis can no longer be limited to inflammasome signaling. GSDMD, GSDME, and other gasdermin family members can also contribute to this cell death. It is considered as a potential pathogenic process for atherosclerosis,[30] diabetes,[31] acute lung injury,[32] and ischemia–reperfusion injury.[33] Recent studies have reported that caspase-3 can also cleave GSDME to generate an N-terminal fragment (N-GSDME) that works for pyroptosis, which shows cleavage of GSDME by caspase-3 induced pyroptosis in certain GSDME-expressing cancer cells after chemotherapy. Our previous study demonstrated that inflammatory caspase-4/11 participated in the PAEC pyroptosis, proving that pyroptosis playing a vital role in the progression of PAH.[20] In our study, we found that pyroptosis is involved in pulmonary arterial endothelium and induced endothelial dysfunction. Inhibiting GSDME is sufficient to alleviate the pathological process of PAH via inhibiting the pyroptosis pathway, which is in consistent with our previous work, strengthening the importance of endothelial pyroptosis in PAH.

Thus, our study illuminated that GSDME-mediated pyroptosis participated in the progression of PAH.

To study how NLRP3/GSDME-mediated pyroptosis is activated in PAH, we assumed that loss of BMPR2 is important for this progression. Bone morphogenetic proteins belong to members of the TGFβ super family, participating in a wide range of developmental processes. The BMPR2 signaling pathway plays a vital role in regulating pulmonary vascular homeostasis. Loss of BMPR2 is responsible for the initiation and progress of hereditary PAH and a proportion of idiopathic PAH. Previous studies have shown that conditional deletion of BMPR2 in the endothelium is sufficient to induce PAH and endothelial BMPR2 expression reverses experimental pulmonary hypertension. Additional studies have identified a role for endothelial BMPR2 loss in the exacerbation of vascular permeability and the altered translocation of leukocytes across the vascular wall.[34] Overall, the dysfunction of BMPR2 signaling plays a critical role during the initiation and progress of PH[35]. However, the precise mechanism of the endothelial BMP signaling in the pathobiology of PAH remains uncertain. BMPR2/smad signaling was dysregulated in monocrotaline-induced PAH.[36] Our laboratory previously demonstrated that HMGB1/TLR4 signaling promotes pulmonary arterial smooth muscle cells migration and proliferation via suppressing canonical BMPR2/smad signaling,[37] illuminating that BMPR2/smad signaling functions in a large variety of physiopathological processes. Besides the canonical SMAD pathway, BMP-receptor activation can also induce non-SMAD signaling. In this study, we focused on investigating the underlying mechanism of BMPR2 deficiency-mediated the inflammatory process in PAECs, finding that BMPR2 deficiency can induce NLRP3 and GSDME activity in experimental PAH models and PAECs. However, reversed BMPR2 activity is sufficient to recover PAH progression; it inhibits the activation of NLRP3 and GSDME, accompanied with decreased IL-1β, suggesting that the NLRP3/GSDME axis acts as downstream of BMPR2 signaling to mediate the inflammatory response in PAH, illustrating a new mechanism of BMPR2/NLRP3/GSDME signaling in PAH. One recent article reported that the lipopolysaccharide-induced pyroptosis exacerbates BMPR2 signaling deficiency in systemic lupus erythematosus-PAH, which illustrated that deficiencies of BMPR2 signaling and pyroptosis-pathway-related proinflammatory factors together contribute to the development of PAH in systemic lupus erythematosus, demonstrating a potential mechanism underlying PAH penetrance in systemic lupus erythematosus. The environmental pathogenic lipopolysaccharide-induced pyroptosis as “second hit” together with deficient BMPR2 signaling pathway, which strengthens our point that BMPR2 was involved in the process of pyroptosis.[38] Moreover, though we have verified that NLRP3 knockout or GSDME inhibition alleviates the progression of PAH in the animal models, implying that NLRP3/GSDME signaling-associated pyroptosis could also be triggered and play a pivotal role in the PAH, whereas in this study, we focusing on investigating the underlying mechanism of BMPR2 deficiency-mediated inflammation. Thus, we did not use gene intervention of NLRP3/GSDME to illustrate whether that signaling has a pivotal role in the PAECs as well as in the PAH animal models, as to how BMPR2 interacts with the NLRP3 pathway, it may involve complicated biological process, which will be explored in depth in our future work.

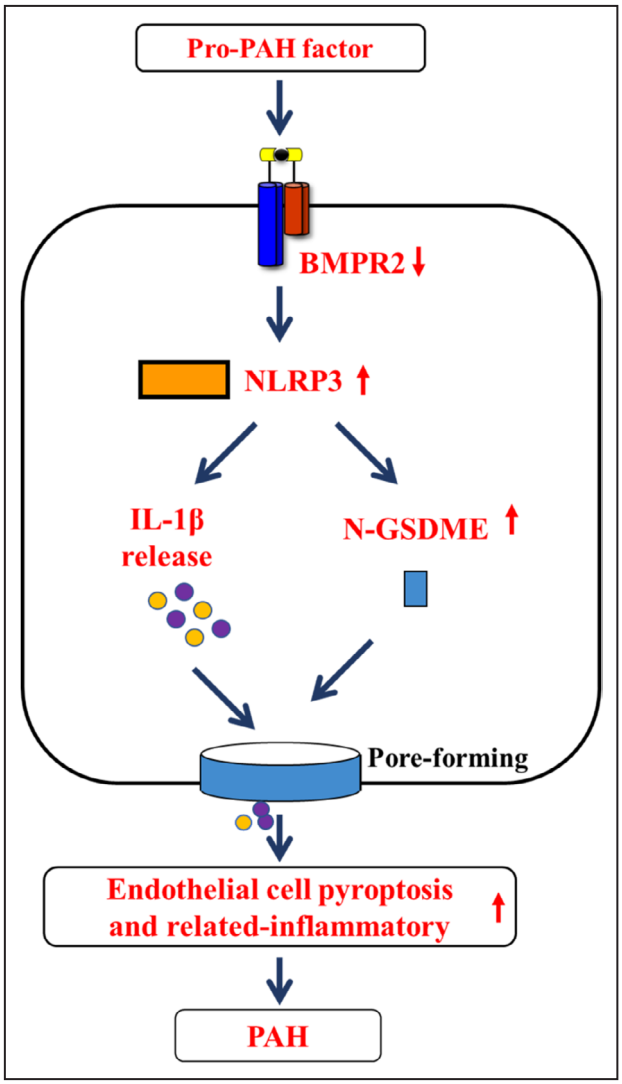

Figure 8. Schematic diagram of the mechanism of NLRP3/GSDME promoting PAH.
BMPR2 indicates type 2 bone morphogenetic protein receptor; GSDME, gasdermin E; IL-1β, interleukin-1β; NLRP3, NOD-like receptor family protein 3; and PAH, pulmonary arterial hypertension.

This study revealed that increased NLRP3 and GSDME were detected in pulmonary hypertension animal models and endothelial cell models with PAH. This indicates that NLRP3 and GSDME potentially act as diagnostic biomarkers and therapeutic targets for PAH. Meanwhile, downregulation of BMPR2 activates NLRP3/GSDME-mediated endothelial pyroptosis, thereby contributing to the promotion of PAH, which authenticates that targeting BMPR2 such as use of FK506 or BMP9 can act as novel therapeutic targets for PAH. Nevertheless, there are some limitations would be taken into account in this study. First, PAH is a complicated disease with different kinds of manifestations. The contribution of NLRP3 and GSDME to the development and progression of human PAH remains largely unknown. Thus, to extrapolate the observations from PAH models to human PAH is still difficult. It is necessary to elucidate the effect of those markers in patients with PAH before considering them as diagnostic biomarkers of PAH. Second, NLRP3 gene systemic knockout mice were used in this study. Endothelial cell-specific NLRP3 knockout mice may help us further understand the role and mechanism of NLRP3 in PAH. Moreover, as the female sex presents a clinically significant risk factor for the development of pulmonary hypertension,[38] considering the difference in the physiological structure of men and women and the different effects sex has on PH, we used only male animals in our study. Third, the specific regulatory interactions between BMPR2 and NLRP3/GSDME necessitate further investigation. Moreover, in the statistic part, some of the group sizes are small, and Shapiro–Wilk test was used for normality, it may be underpowered. This is a limitation of this work; we will enlarge the sample size in our next study.

Conclusions

In summary, the present study shows NLRP3 knockout or inhibition of GSDME attenuates the development of PAH (Figure 8). Meanwhile, it demonstrates for the first time that loss of BMPR2 promotes NLRP3/GSDME-meditated pyroptosis to induce inflammatory response in PAH, which provides a novel mechanistic view into BMPR2 deficiency and may offer new targets for PAH treatment.

ARTICLE INFORMATION

Received January 28, 2024; accepted December 13, 2024.

Affiliations

The Center for Vascular Disease and Translational Medicine, The Third Xiangya Hospital (X-t.T., Z-y.P., Y-s.W., A.F.C., X-h.L.) and , Department of Pharmacology, Xiangya School of Pharmaceutical Science (X-t.T., Y-y.C., X-h.L.), Central South University, Changsha, ChinaHunan Key Laboratory for Bioanalysis of Complex Matrix Samples, Changsha, China (X-t.T., Y-y.C., Y.L., X-h.L.); Department of Health Management Center, The Third Xiangya Hospital, Central South University, Changsha, China (Z-y.P., Y.L.); Key Laboratory of Study and Discovery of Small Targeted Molecules of Hunan, School of Medicine, Hunan Normal University, Changsha, China (Y-s.W.); Institute for Developmental and Regenerative Cardiovascular Medicine, Xinhua Hospital, Shanghai Jiao Tong University School of Medicine, Shanghai, China (X-c.L., A.F.C.); and Xiangya Nursing School, Central South University, Changsha, China (S-Y.T.).

Acknowledgments

The NLRP3$^{-/-}$ mice were a kind gift from Professor Ben Lu at the Central South University.

Sources of Funding

This work was supported in part by grants from the Ministry of Science and Technology of China (2021YFA0804803, 2022YFA1104204), the Natural Science Foundation of China (82 495 172, 82 421 001, 82 241 027), Hunan Young Talent grant (2020RC3063), Hunan Science Foundation (2020JJ5864, 2021JJ10071, 2024JJ6327) and the Wisdom Accumulation and Talent Cultivation Project of the Third XiangYa Hospital of Central South University (YX202002).

Disclosures

None.

REFERENCES

1. Ranchoux B, Harvey LD, Ayon RJ, Babicheva A, Bonnet S, Chan SY, Yuan JX, Perez VJ. Endothelial dysfunction in pulmonary arterial hypertension: an evolving landscape (2017 Grover conference series). *Pulm Circ*. 2018;8:2045893217752912. doi: 10.1177/2045893217752912
2. Yang X, Long L, Southwood M, Rudarakanchana N, Upton PD, Jeffery TK, Atkinson C, Chen H, Trembath RC, Morrell NW. Dysfunctional Smad signaling contributes to abnormal smooth muscle cell proliferation in familial pulmonary arterial hypertension. *Circ Res*. 2005;96:1053–1063. doi: 10.1161/01.RES.0000166926.54293.68
3. Noordegraaf AV, Westerhof BE, Westerhof N. The relationship between the right ventricle and its load in pulmonary hypertension. *J Am Coll Cardiol*. 2017;69:236–243. doi: 10.1016/j.jacc.2016.10.047
4. Aldred MA, Vijayakrishnan J, James V, Soubrier F, Gomez-Sanchez MA, Martensson G, Galie N, Manes A, Corris P, Simonneau G, et al. Gene rearrangements account for a significant proportion of mutations in familial and idiopathic pulmonary arterial hypertension. *Hum Mutat*. 2006;27:212–213. doi: 10.1002/humu.9398
5. Frump A, Prewitt A, de Caestecker MP. Mutations and endothelial dysfunction in pulmonary arterial hypertension (2017 Grover conference series). *Pulmonary Circulation*. 2018;8:2045894018765840. doi: 10.1177/2045894018765840
6. Long L, Ormiston ML, Yang XD, Southwood M, Gräf S, Machado RD, Mueller M, Kinzel B, Yung LM, Wilkinson JM, et al. Selective enhancement of endothelial BMPR-II with BMP9 reverses pulmonary arterial hypertension. *Nat Med*. 2015;21:777–785. doi: 10.1038/nm.3877
7. Spiekerkoetter E, Tian XF, Cai J, Hopper RK, Sudheendra D, Li CYG, El-Bizri N, Sawada H, Haghighat R, Chan R, et al. FK506 activates BMPR2 rescues endothelial dysfunction, and reverses pulmonary hypertension. *J Clin Invest*. 2013;123:3600–3613. doi: 10.1172/JCI65592
8. Benn A, Bredow C, Casanova I, Vukicevic S, Knaus P. VE-cadherin facilitates BMP-induced endothelial cell permeability and signaling. *J Cell Sci*. 2016;129:206–218. doi: 10.1242/jcs.179960
9. Rabinovitch M, Guignabert C, Humbert M, Nicolls MR. Inflammation and immunity in the pathogenesis of pulmonary arterial hypertension. *Circ Res*. 2014;115:165–175. doi: 10.1161/CIRCRESAHA.113.301141
10. Libby P, Hansson GK. Inflammation and immunity in diseases of the arterial tree players and layers. *Circ Res*. 2015;116:307–311. doi: 10.1161/CIRCRESAHA.116.301313
11. Hurst LA, Dunmore BJ, Long L, Crosby A, Al-Lamki R, Deighton J, Southwood M, Yang XD, Nikolic MZ, Herrera B, et al. TNFα drives pulmonary arterial hypertension by suppressing the BMP type-II receptor and altering NOTCH signalling. *Nat Commun*. 2017;8:14079. doi: 10.1038/ncomms14079
12. Wang Q, Zuo XR, Wang YY, Xie WP, Wang H, Zhang MJ. Monocrotaline-induced pulmonary arterial hypertension is attenuated by TNF-α antagonists via the suppression of TNF-α expression and NF-κB pathway in rats. *Vascul Pharmacol*. 2013;58:71–77. doi: 10.1016/j.vph.2012.07.006

13. Soon E, Crosby A, Southwood M, Yang P, Tajsic T, Toshner M, Appleby S, Shanahan CM, Bloch KD, Pepke-Zaba J, et al. Bone morphogenetic protein receptor type II deficiency and increased inflammatory cytokine production. *Am J Resp Crit Care*. 2015;192:859–872. doi: 10.1164/rccm.201408-1509OC
14. Wang J, Tian XT, Peng Z, Li WQ, Cao YY, Li Y, Li XH. HMGB1/TLR4 promotes hypoxic pulmonary hypertension via suppressing BMPR2 signaling. *Vascul Pharmacol*. 2019;117:35–44. doi: 10.1016/j.vph.2018.12.006
15. Ozaki E, Campbell M, Doyle SL. Targeting the NLRP3 inflammasome in chronic inflammatory diseases: current perspectives. *J Inflamm Res*. 2015;8:15–27. doi: 10.2147/JIR.S51250
16. Shi J, Gao W, Shao F. Pyroptosis: Gasdermin-mediated programmed necrotic cell death. *Trends Biochem Sci*. 2017;42:245–254. doi: 10.1016/j.tibs.2016.10.004
17. Kovacs SB, Miao EA. Gasdermins: effectors of Pyroptosis. *Trends Cell Biol*. 2017;27:673–684. doi: 10.1016/j.tcb.2017.05.005
18. Ding J, Wang K, Liu W, She Y, Sun Q, Shi J, Sun H, Wang DC, Shao F. Pore-forming activity and structural autoinhibition of the gasdermin family. *Nature*. 2016;535:111–116. doi: 10.1038/nature18590
19. Rogers C, Fernandes-Alnemri T, Mayes L, Alnemri D, Cingolani G, Alnemri ES. Cleavage of DFNA5 by caspase-3 during apoptosis mediates progression to secondary necrotic/pyroptotic cell death. *Nat Commun*. 2017;8:14128. doi: 10.1038/ncomms14128
20. Wu Y, Pan B, Zhang Z, Li X, Leng Y, Ji Y, Sun K, Chen AF. Caspase-4/11-mediated pulmonary artery endothelial cell Pyroptosis contributes to pulmonary arterial hypertension. *Hypertension*. 2022;79:536–548. doi: 10.1161/HYPERTENSIONAHA.121.17868
21. Zhang J, He Y, Yan X, Chen S, He M, Lei Y, Zhang J, Gongol B, Gu M, Miao Y, et al. MicroRNA-483 amelioration of experimental pulmonary hypertension. *EMBO Mol Med*. 2020;12:e11303. doi: 10.15252/emmm.201911303
22. Li T, Zha L, Luo H, Li S, Zhao L, He J, Li X, Qi Q, Liu Y, Yu Z. Galectin-3 mediates endothelial-to-mesenchymal transition in pulmonary arterial hypertension. *Aging Dis*. 2019;10:731–745. doi: 10.14336/AD.2018.1001
23. Miao H, Qiu F, Zhu L, Jiang B, Yuan Y, Huang B, Zhang Y. Novel angiogenesis strategy to ameliorate pulmonary hypertension. *J Thorac Cardiovasc Surg*. 2021;161:e417–e434. doi: 10.1016/j.jtcvs.2020.03.044
24. Craven RR, Gao X, Allen IC, Gris D, Bubeck Wardenburg J, McElvania-Tekippe E, Ting JP, Duncan JA. Staphylococcus aureus alpha-hemolysin activates the NLRP3-inflammasome in human and mouse monocytic cells. *PLoS One*. 2009;4:e7446. doi: 10.1371/journal.pone.0007446
25. Duncan JA, Gao X, Huang MT, O'Connor BP, Thomas CE, Willingham SB, Bergstralh DT, Jarvis GA, Sparling PF, Ting JP. Neisseria gonorrhoeae activates the proteinase cathepsin B to mediate the signaling activities of the NLRP3 and ASC-containing inflammasome. *J Immunol*. 2009;182:6460–6469. doi: 10.4049/jimmunol.0802696
26. Greaney AJ, Portley MK, O'Mard D, Crown D, Maier NK, Mendenhall MA, Mayer-Barber KD, Leppla SH, Moayeri M. Frontline science: anthrax lethal toxin-induced, NLRP1-mediated IL-1β release is a neutrophil and PAD4-dependent event. *J Leukoc Biol*. 2020;108:773–786. doi: 10.1002/JLB.4HI0320-028R
27. Wang HY, Lv CE, Wang S, Ying HJ, Weng YS, Yu WJ. NLRP3 inflammasome involves in the acute exacerbation of patients with chronic obstructive pulmonary disease. *Inflammation*. 2018;41:1321–1333. doi: 10.1007/s10753-018-0780-0
28. Shi JJ, Zhao Y, Wang K, Shi XY, Wang Y, Huang HW, Zhuang YH, Cai T, Wang FC, Shao F. Cleavage of GSDMD by inflammatory caspases determines pyroptotic cell death. *Nature*. 2015;526:660–665. doi: 10.1038/nature15514
29. Wang YP, Gao WQ, Shi XY, Ding JJ, Liu W, He HB, Wang K, Shao F. Chemotherapy drugs induce pyroptosis through caspase-3 cleavage of a gasdermin. *Nature*. 2017;547:99–103. doi: 10.1038/nature22393
30. Xu YJ, Zheng L, Hu YW, Wang Q. Pyroptosis and its relationship to atherosclerosis. *Clin Chim Acta*. 2018;476:28–37. doi: 10.1016/j.cca.2017.11.005
31. Yu ZW, Zhang J, Li X, Wang Y, Fu YH, Gao XY. A new research hot spot: the role of NLRP3 inflammasome activation, a key step in pyroptosis, in diabetes and diabetic complications. *Life Sci*. 2020;240:117138. doi: 10.1016/j.lfs.2019.117138
32. Li DD, Ren WY, Jiang ZL, Zhu L. Regulation of the NLRP3 inflammasome and macrophage pyroptosis by the p38 MAPK signaling pathway in a mouse model of acute lung injury. *Mol Med Rep*. 2018;18:4399–4409. doi: 10.3892/mmr.2018.9427
33. Toldo S, Mauro AG, Cutter Z, Abbate A. Inflammasome, pyroptosis, and cytokines in myocardial ischemia-reperfusion injury. *Am J Physiol-Heart C*. 2018;315:H1553–H1568. doi: 10.1152/ajpheart.00158.2018
34. Vengethasamy L, Hautefort A, Tielemans B, Belge C, Perros F, Verleden S, Fadel E, Van Raemdonck D, Delcroix M, Quarck R. BMPRII influences the response of pulmonary microvascular endothelial cells to inflammatory mediators. *Pflug Arch Eur J Phy*. 2016;468:1969–1983. doi: 10.1007/s00424-016-1899-1
35. Hautefort A, Mendes-Ferreira P, Sabourin J, Manaud G, Bertero T, Rucker-Martin C, Riou M, Adao R, Manoury B, Lambert M, et al. Mutant rats develop pulmonary and cardiac characteristics of pulmonary arterial hypertension. *Circulation*. 2019;139:932–948. doi: 10.1161/CIRCULATIONAHA.118.033744
36. Morty RE, Nejman B, Kwapiszewska G, Hecker M, Zakrzewicz A, Kouri FM, Peters DM, Dumitrascu R, Seeger W, Knaus P, et al. Dysregulated bone morphogenetic protein signaling in monocrotaline-induced pulmonary arterial hypertension. *Arterioscl Throm vas*. 2007;27:1072–1078. doi: 10.1161/ATVBAHA.107.141200
37. Xing YJ, Zhao JL, Zhou MJ, Jing SL, Zhao X, Mao P, Qian JN, Huang C, Tian Z, Wang Q, et al. The LPS induced pyroptosis exacerbates BMPR2 signaling deficiency to potentiate SLE-PAH. *FASEB J*. 2021;35:e22044. doi: 10.1096/fj.202100851RR
38. Nie C, Zhu Y, Xiao M, Zhu C, Meng Y, Lu Z, Yang Q, Wang S. Sex differences in the prevalence and survival of pulmonary hypertension in obstructive hypertrophic cardiomyopathy following septal myectomy. *Int J Cardiol Heart Vasc*. 2025;56:101569. doi: 10.1016/j.ijcha.2024.101569